

# Homogenization and trend analysis of 1960–2015 *in situ* sea surface temperature observations along the coast of China

Yan Li<sup>1, 2</sup>, Qingyuan Wang<sup>3</sup>, Guoyu Ren<sup>4, 5</sup>, Guosong Wang<sup>6</sup>, Qingliang Zhou<sup>7\*</sup>

<sup>1</sup> College of Life Sciences and Oceanography, Shenzhen University, Shenzhen 518061, China

<sup>2</sup> Southern Marine Science and Engineering Guangdong Laboratory (Guangzhou), Guangzhou 511458, China

<sup>3</sup> Tianjin Meteorological Observatory, Tianjin 300074, China

<sup>4</sup> School of Environmental Studies, China University of Geosciences, Wuhan 430074, China

<sup>5</sup> National Climate Center, Beijing 100081, China

<sup>6</sup> National Marine Data and Information Service, Tianjin 300171, China

<sup>7</sup> National Meteorological Center, Beijing 100081, China

Received 13 March 2020; accepted 21 July 2020

© Chinese Society for Oceanography and Springer-Verlag GmbH Germany, part of Springer Nature 2021

## Abstract

Sea surface temperature (SST) measurements from 26 coastal hydrological stations of China during 1960–2015 were homogenized and analyzed in this study. The homogenous surface air temperature (SAT) series from meteorological stations which were highly correlated to SST series was used to construct the reference series. Monthly mean SST series were then derived and subjected to a statistical homogeneity test, called penalized maximal *t* test. Homogenized monthly mean SST series were obtained by adjusting all significant change points which were supported by historic metadata information. Results show that the majority of break points are caused by instrument change and station relocation, which accounts for about 61.3% and 24.2% of the total break points, respectively. The regionally averaged annual homogeneous SST series from the 26 stations shows a warming trend (0.19°C per decade). This result is consistent with that based on the homogenized annual mean SAT at the same region (0.22°C per decade), while the regionally averaged mean original SST series from the same stations shows a much weaker warming of 0.09°C per decade for 1960–2015. This finding suggests that the effects of artificial change points on the result of trend analysis are remarkable, and the warming rate from original SST observations since 1960 may be underestimated. Thus a high quality homogenized observation is crucial for robust detection and assessment of regional climate change. Furthermore, the trends of the seasonal mean homogenized SST were also analyzed. This work confirmed that there was an asymmetric seasonal temperature trends in the Chinese coastal water in the past decades, with the largest warming rate occurring in winter. At last, the significant warming in winter and its relationships to the variability of three large-scale atmospheric modes were investigated.

**Key words:** SST, homogenization, observation system changes, penalized maximal *t* test

**Citation:** Li Yan, Wang Qingyuan, Ren Guoyu, Wang Guosong, Zhou Qingliang. 2021. Homogenization and trend analysis of 1960–2015 *in situ* sea surface temperature observations along the coast of China. Acta Oceanologica Sinica, 40(5): 36–46, doi: 10.1007/s13131-021-1725-2

## 1 Introduction

Global warming places shallow water ecosystems at more risk than those in the open ocean as their temperatures may change more rapidly and dramatically (Belkin, 2009; Stramska and Białogrodzka, 2015). In the 21st century, offshore areas of the northern Pacific Ocean are expected to be some of the prominent and vulnerable climate change “hot spots” (Lima and Wethey, 2012; Frölicher and Laufkötter, 2018). As a part of the Northwest Pacific Ocean, the seas adjacent of Chinese mainland including the Bohai Sea, the Yellow Sea, the East China Sea and the South China Sea (Fig. 1) are also sensitive to the effects of natural and anthropogenic climate changes (Halpern et al., 2008; Cai et al., 2016). It is therefore necessary to give an accurate assessment of the trend of water temperature.

The National Marine Observation System along the coast of

China has been set up and gradually improved since 1960. Among them, there are 26 hydrological observing stations with long-term (exceeding 50 years) and continuous *in situ* sea surface temperature (SST) observations. Yet, studies have found that these long-term observations contain several spurious changes and artificial change points suffering from station relocation, instrument change, transformation of observing system and so on, which are prone to systematic errors or biases (Li et al., 2009; Xu et al., 2013; Hausfather et al., 2016; Minola et al., 2016; Yang et al., 2018). SST records from coastal hydrological stations of China are no exception (Li et al., 2016). Therefore, it is necessary to homogenize the historical observational data in order to monitor, detect and assess the long-term change in climate and environment in the Chinese coastal waters.

In the study, monthly mean SST series from 26 coastal hydro-

Foundation item: The Shenzhen Fundamental Research Program under contract No. JCYJ20200109110220482; the Special Project for Introduced Talents Team of Southern Marine Science and Engineering Guangdong Laboratory (Guangzhou) under contract No. GML2019ZD0604; the Shenzhen University Stability Support Program under contract No. 20200810000724001.

\*Corresponding author, E-mail: zhouql@cma.gov.cn

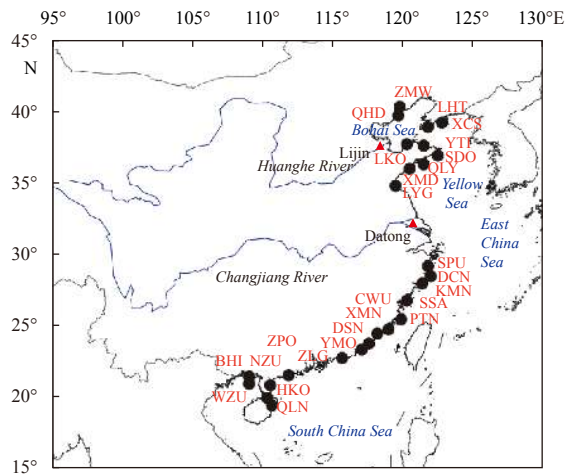


**Fig. 1.** Locations of the 26 coastal hydrological stations at the Chinese coast (black dots). Red triangles represent two gauge stations (Lijin and Datong) used in the study. The China coasts are divided into the coasts of Chinese mainland in the Bohai Sea, Yellow Sea, East China Sea and South China Sea. The full names of the stations are shown in Table 1.

logical stations for 1960–2015 were homogenized, using available metadata information and statistical homogeneity method. Then, the homogenized SST series were used to assess the oceanic climate change in the coastal waters at annual and seasonal scales. Results should potentially enable us to more accurately detect the magnitude of SST warming rate in this region. SST variability is governed by both atmospheric and oceanic processes (Deser et al., 2010). This work further studied the possible influence of large-scale atmospheric circulations on the observed SST variability across China.

The structure of the paper is arranged as follows. Data and metadata from coastal hydrological stations are described in Section 2. A brief introduction to methods of detecting and inhomogeneity adjustment is given in Section 3. Section 4 reports the statistics of detected change points and related causes, the inhomogeneity impacts on the long-term trends, and the trends of seasonal mean SST and possible influence of large-scale atmospheric circulation on the winter SST trends. At the end, discussion and conclusions are given in Section 5.

## 2 Data

### 2.1 Sea surface temperature, surface air temperature and metadata

Currently, more than 100 hydrological stations are being op-

erated and run. Among these stations, only 26 stations have taking routine and continuous measurements since 1960 (Table 1), with the percentage of missing data lower than 4%. These observed data series have undergone the least relocation (no more than 5 relocations reported by the available metadata). All of these data are provided by the National Marine Data and Information Service of China and can be obtained in the National Science & Technology Resource Sharing Service Platform of China (<http://mds.nmdis.org.cn>). The locations of these stations are shown in Fig. 1. There are few stations at the southern Yellow Sea, because the coast area is a vast beach and salinized land which is not suitable for hydrological stations. Since the 2000s, there have been only some automatic stations. These measurements have been quality controlled, including the checks in climatological limit, gradient, the temporal and spatial consistency and so on, according to the codes from *The Specification for Off-shore Observations* (People's Republic of China National Bureau of Technical Supervision, 2006) (<http://www.std.gov.cn/gb/gbQuery>). Monthly mean SST was calculated from the average of each daily mean SST in a month. Following the method of Wan et al. (2010) and Azorin-Molina et al. (2014), monthly means have been calculated for months with at least 26 days of observations. Otherwise the whole month has been set as missing. Then the data in some missing months are reconstructed by the neighbor data using linear regression analysis method.

Metadata information of each coastal hydrological station was used to verify the statistically detected change points, including the station coordinates, height, instrument change, station relocation, environment change, algorithms for calculating a daily mean, observing procedures, observation system change, etc. All of the metadata information was documented in standard files, called "Hydrological Station History Data Files". The homogeneous monthly mean surface air temperature (SAT) series from National Meteorological Information Center of China Meteorological Administration were used to construct reference series which have significant relationship with SST series (Xu et al., 2013).

### 2.2 OISST

A globally gridded SST dataset with high resolution is used in this work for comparative analysis of SST series for the region in the present study. The  $0.25^\circ \times 0.25^\circ$  NOAA Optimum Interpolation SST (OISST) version 2 using Advanced Very High-Resolution Radiometer infrared satellite SST data from the Pathfinder satellite combined with buoy data, ship data, and sea ice data, covering from 1982 to 2015 (Reynolds et al., 2007), are available at <http://www.ncdc.noaa.gov/oisst>.

### 2.3 Three atmospheric circulation indices

Three atmospheric circulation indices, (1) the Arctic Oscilla-

**Table 1.** The 26 coastal hydrological stations used in the study

Station	Abbreviation	Station	Abbreviation	Station	Abbreviation
Zhimaowan	ZMW	Lianyungang	LYG	Yunwo	YWO
Qinhuangdao	QHD	Shipu	SPU	Zhelang	ZLG
Xiaochangshan	XCS	Dachen	DCN	Zapo	ZPO
Laohutan	LHT	Kaimen	KMN	Beihai	BHI
Longkou	LKO	Sansha	SSA	Weizhou	WZU
Yantai	YTI	Pintan	PTN	Naozhou	NZU
Shidao	SDO	Congwu	CWU	Haikou	HKO
Qianliyan	QLY	Xiamen	XMN	Qinlan	QLN
Xiaomaidao	XMD	Dongshan	DSN		

tion (AO) index, (2) the East Asian Trough (EAT) index, and (3) the North Pacific Oscillation (NPO) index, were used to analyze the possible influence of large-scale atmospheric circulation on the winter SST variability along the Chinese coast. The AO, EAT and NPO are considered the main modes for winter climate variability across the Chinese mainland (Hansen et al., 2010; You et al., 2013; Chen et al., 2013; Sun et al., 2018) and the SST variability over the China seas (Zhang et al., 2010; Yeh and Kim, 2010; Huang et al., 2016; Li et al., 2015; Pei et al., 2017; Cai et al., 2017); therefore, their possible influence on near-shore SST trends has been investigated in this study.

AO index is defined as the first leading mode from the empirical orthogonal function (EOF) analysis of monthly mean height anomalies at 1 000 hPa (Northern Hemisphere) (Thompson and Wallace, 1998). The AO index series has been obtained from the National Oceanic and Atmospheric Administration (NOAA) (available online at <https://www.esrl.noaa.gov/psd/data/correlation/ao.data>). The definition of EAT index adopted here is the one defined by Sun and Li (1997); that is, the EAT index is the normalized 500 hPa geopotential heights averaged over the area (25°–45°N, 110°–145°E). NPO index is defined as the principal component of the second mode of analysis for the standardized winter sea level pressure (SLP) over the North Pacific (20°–80°N, 120°E–120°W) (Linkin and Nigam, 2008). Monthly mean 500 hPa geopotential heights and SLP used to calculate EAT index and NPO index in the study is obtained from the National Centers for Environmental Prediction/National Center for Atmospheric Research reanalysis (downloaded from <http://www.cdc.noaa.gov>) (Kalnay et al., 1996).

### 3 Homogenization method and statistical analysis methods

#### 3.1 Homogenization method

It is a common practice to use a statistical method to detect break points in long-term series, and rely on metadata for break point determination. Several homogenization algorithms have been identified and assessed in recent years (Reeves et al., 2007; Ribeiro et al., 2015). Among them, the PMTred algorithm is based on the penalized maximal  $t$  (PMT) test for searching for the most probable position of shift in a segment of the series being tested and tests its statistical significance using a penalized maximal  $t$  test statistic, in which the lag-1 autocorrelation is also accounted for (Wang, 2008a). PMTred methods have three advantages comparing to other techniques: (1) PMTred accounts for the effects of unequal lengths of the two segments before and after a shift and thereby has higher detection power (Wang et al., 2007); (2) PMTred has a re-recursive testing procedure for detecting multiple change points in a single time series, and (3) PMTred accounts for lag-1 autocorrelation which are often non-negligible for climate data time series and thereby reduces the number of false alarms (Wang, 2008b). The PMTred algorithm is implemented using the RHtest V4 software package (Wang and Feng, 2013). This package includes plots of the relevant time series and the

resulting estimate of shifts and trends in the candidate series, which are convenient for its user. RHtest V4 and its previous versions developed have been widely used in homogenizing climate data (Wan et al., 2010; Kuglitsch et al., 2012; Vincent et al., 2012; Xu et al., 2013). Thus, PMT test based algorithm is also applied to detect non-climatic change points in monthly mean SST time series. Because the time series being tested is assumed to have no temporal trends, the PMTred algorithm needs to use a reference series to represent trends and low frequency variations in the candidate series. There are two steps to detect these non-climatic change points.

##### 3.1.1 Construction of reference series

Generally, the most common way to construct reference series is to use a data series from nearby stations for a candidate series (a series to be tested and homogenized). However, this is not appropriate for SST series, because the coastal hydrological stations along the coast of China are sparse and not evenly. Besides, all of the stations have experienced a transformation from manual observation system to automatic observation system, during the early 2000s. These facts increase the difficulty of establishing reference series based on SST series from nearby hydrological stations. Thus, homogeneous SAT series was used to construct a reference series for each SST series, because SAT series from neighboring meteorological stations well represent the same climatic variations as the SST in the coastal areas of China (Sun, 2006). The proposed method above has been used in previous studies. For instance, Stephenson et al. (2008) systematically detected the inhomogeneities in the SAT series of Caribbean and adjacent Caribbean using neighboring SST series. The procedure of reference series construction in this article is referred. These homogenized SAT series from meteorological stations have been selected because they met all of the following selection criteria in Table 2. Then, the homogenous monthly SAT series which are well correlated with the SST series are used to construct reference series by correlation coefficient weighted average method.

##### 3.1.2 Verification of the change points and the adjustment

Homogeneities of the 26 monthly SST series have been tested by applying PMT test. PMT test detects all the possible inhomogeneities at a statistically significance level of 5%—these detected break points which are confirmed by metadata have been homogenized. These detected break points are considered to be a real one only when metadata indicate a documented change within 1 year before or after the date of change point detected by PMT and identified to be a documented break point. The documented time of change is used to replace the estimated time of change when they are not identical (due to estimation error). The break points which cannot be validated by the metadata are kept as they are.

The objective of the quantil-matching (QM) adjustment is to adjust the series to that the empirical distributions of all segments of the de-trended base series match each other, the adjustment value depends on the empirical frequency of the datum to

**Table 2.** Criteria for selecting the reference meteorological stations

Number	Criteria
1	The horizontal distance between candidate coastal hydrological station and reference meteorological stations should be within 100 km, in term of the geographical distribution
2	Correlation coefficient between the annual mean original SST series and the annual mean homogeneous SAT series should be equal to or higher than 0.7, following with the previous research (Malcher and Schönwiese, 1987). And only in this case, the reference series can represent at least 50% the variability in the candidate series (Malcher and Schönwiese, 1987; Stephenson et al., 2008)
3	In order to reduce the urban heat island effect on SAT series, the selected meteorological observing stations are located at rural, towns or middle-size cities, rather than big cities according to Ren et al. (2010)

be adjusted. As a result, the shape of the distribution is often adjusted, although the tests are meant to detect mean-shifts. Importantly, the annual cycle, lag-1 autocorrelation, and linear trend of the base series were estimated in tandem while accounting for all identified shifts (Wang, 2008a); and the trend component estimated for the base series is preserved in the QM adjustment algorithm (Wang et al., 2010).

### 3.2 Statistical analysis method

The linear trends in the raw and homogenized SST during 1960–2015 are estimated via the least-squares linear fitting method. The significance of each trend also has been tested. Here the Mann-Kendall test for trends and Sen's slope estimates are used to detect and quantify trends (Sen, 1968), with magnitudes of trends and slopes assessed at the 0.05 significance level ( $p < 0.05$ ).

## 4 Results

### 4.1 Detected break points and their causes

Figure 2 shows an example of applying PMT test to the monthly mean SST series of BHI hydrological station, which is located at the coast of the South China Sea. March 2005 was identified as a highly significant break point ( $PT_{\max} = 6.92 > 3.71$ , the upper bound of the corresponding 95-th percentile of  $PT_{\max}$ ), which is easily visible in Fig. 2a. According to the historic metadata information of BHI station, the observing practice was transformed from manual observation system to automatic observation system and the instrument was changed from SWY1-1 Thermometer to ZYZ4-1 Thermohaline Sensor on May 18, 2005. The estimated time (March 2005) of breakpoint in the monthly mean series is 2 months earlier than the actual time documented in the metadata. Then, the estimated time was replaced by the actual time to calculate the final adjustment for this breakpoint. After change points are identified, homogenized monthly mean SST series can be obtained by adjusting the significant shifts caused by documented break points. The QM adjustment method which also combined in RHtest V4 was used to adjust these shifts in the 26 SST series. The SST series of BHI hydrological station was adjusted to the most recent segment by adding  $-0.35$  to all data before May 2005. Here the value  $-0.35$  was calculated from QM method. The homogenized monthly mean series is shown in Fig. 2b.

To summarize, a total of 68 break points have been detected at the 26 monthly SST series for 1960–2015 by PMT method at the significance level of 5%. The statistical break points were identified by metadata. Results show that 62 statistical break points coincide with dates of metadata within  $\pm 1$  year and are referred to as documented break points. Only 10% statistical break points cannot be identified by available metadata. Since 2001, the coastal hydrological stations have experienced a transformation from artificial observing system to automatic observing system, and 15 change points are detected in the year of 2002 (Fig. 3a). Instrument change (including the observing times change caused by the observing system change) is the main cause of break points in monthly SST series. It is responsible for about 61.3% of the total documented break points. Station relocation is found to be the other main cause for discontinuities, accounting for 24.2%. Environmental change and human errors or instrumental malfunctions are the other causes, accounting for 6.4% and 8.1%, respectively (Fig. 3b). Clearly, one or more documented break points are common in the SST series of each station. Series with more than 3 break points are mainly at the coast of the Bohai Sea and the southern East China Sea (Fig. 3b).

Whereas instrument change, station relocation and other changes at observing sites can cause either a rise or a drop in the observed temperatures, the magnitude of all artificial changes is not necessarily symmetrical about zero. For each series, the series to the most recent segment was adjusted by adding  $\Delta$ SST to the data before the documented break points in each series. Here,  $\Delta$ SST is the shift size estimated by QM method. Statistical results show that the  $\Delta$ SST values range from  $-1.2^\circ\text{C}$  to  $1.0^\circ\text{C}$ . The larger portion is the negative adjustments, about 62%. Positive adjustments are responsible for the remaining 38%.

### 4.2 Inhomogeneity impacts on estimated annual mean SST trend

In this subsection, XCS hydrological station, which belongs to the Bohai Sea, was taken as an example to show the influence of break points on estimation of annual mean trend. According to metadata, XCS hydrological station has changed the type of thermometers for three times since 1960. The first change was on January 1, 1965. Only the instrument was changed. The second change was on January 1, 2002. The observing practice was transformed from artificial observation system to automatic observa-

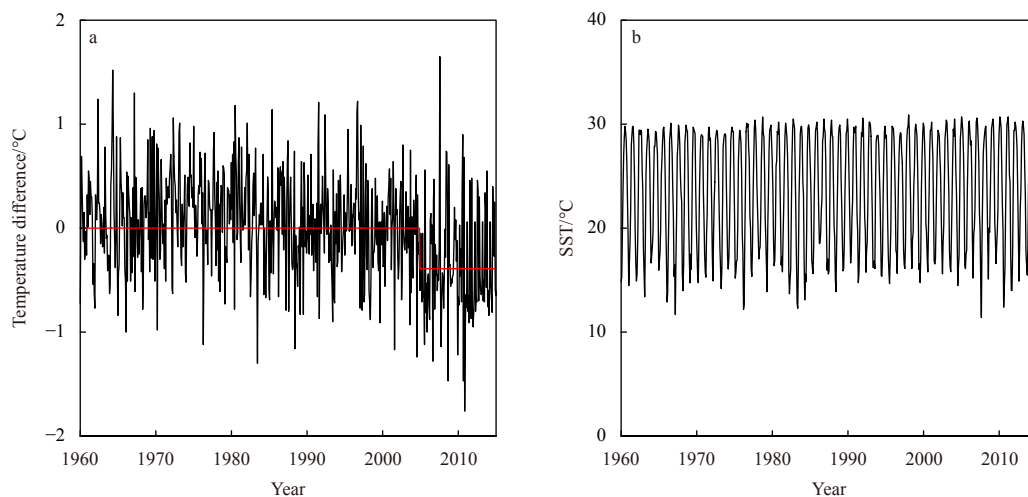
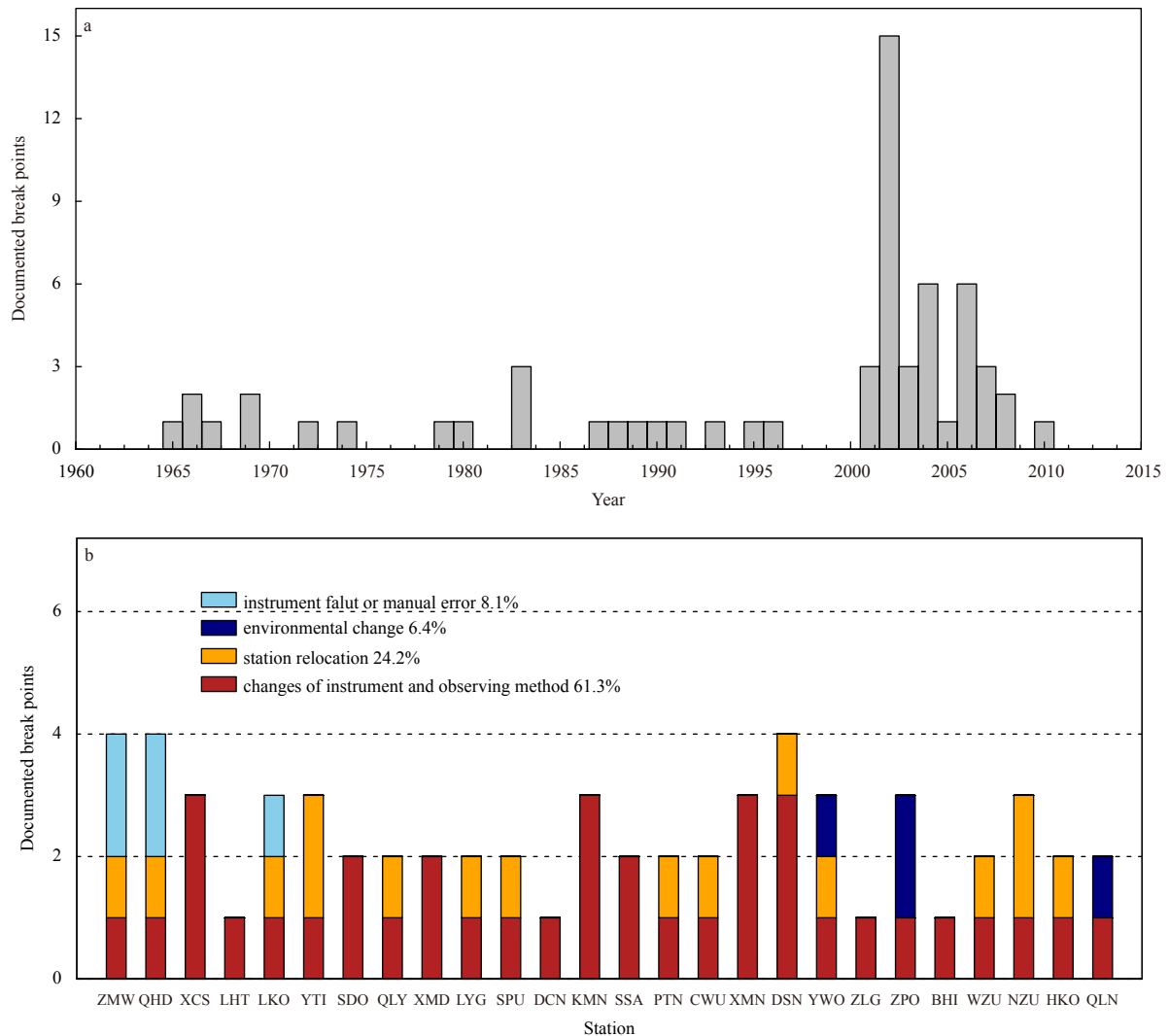


Fig. 2. Monthly mean de-seasonalized SST series with its mean annual cycle subtracted BHI coastal hydrological station (black line; Red line represents the estimated mean response along with the estimated mean shift) (a), and monthly mean homogenized SST series of BHI coastal hydrological station (b).



**Fig. 3.** The total number of identified break points in the 26 SST series of each year from 1960–2015 (a) and the identified break points in SST series of each station (b). See Table 1 and Fig. 1 for the full names and locations of the 26 coastal hydrological stations.

tion system. In the artificial observing period, bucket was used to sample and SST was recorded three times at 08:00, 14:00 and 20:00 UTC by SWY1-1 Thermometer. In the automatic observing period, the observation instrument YZY4-1 Thermohaline Sensor was installed in the thermohaline recorder wells and fixed at the height of 0.5 m below sea level. The SST was recorded every hour. The last change was on July 1, 2004 and the only change is from YZY4-1 Thermohaline Sensor to SWL1-1 Thermometer. The three change points at January 1965, January 2002, and July 2004 introduced three SST shifts of about  $-1.2^{\circ}\text{C}$ ,  $-0.5^{\circ}\text{C}$ , and  $0.36^{\circ}\text{C}$  in the monthly mean series, respectively. Compared to the warming rate of the homogenized SST series for 1960–2015, the raw SST series underestimated the warming rate ( $0.27^{\circ}\text{C}$  per decade vs.  $0.18^{\circ}\text{C}$  per decade). This example illustrates that inhomogeneities caused by artificial reasons can weaken the long-term trends in this region. The result is similar to the conclusions in previous studies of SAT series in China (Cao et al., 2013; Xu et al., 2013; Zhang et al., 2014), despite the causes for the impact of inhomogeneities of the SAT and SST data may be different (Zhang et al., 2014).

For each of the SST measuring sites, there is at least one meteorological station within 100 km distance, according to Table 2.

Such a meteorological station which SAT series had the highest correlation with the SST series of hydrological station was selected, and form 26 pairs of SST/SAT data. Figure 4 displays the regionally averaged raw SST, homogenized SST and the homogenized SAT series (Xu et al., 2013) from 1960 to 2015. The linear trends for 1960–2015 with 95% confidence interval of raw SST series was  $(0.09 \pm 0.06)^{\circ}\text{C}$  per decade, while the linear trend of the homogenized SST are increased to  $(0.19 \pm 0.06)^{\circ}\text{C}$  per decade. The daily and monthly mean SST in the automatic observing period was cooler than that in the artificial observing period (Li et al., 2020). Also, in the study, the correction values of manual transfer were mainly negative. For SST series of each station, the series to the most recent segment was adjusted by adding  $\Delta\text{SST}$  to the data before the documented change points. Finally, the homogenized monthly SST series was obtained. And the homogenized SST largely corrects the warm biases caused by earlier artificial observing. Consequently, the trend from adjusted data is much higher than that of the raw data and the original SST observation is underestimated. Thus, as shown in Fig. 4, the main differences between the raw and homogenized SST series appeared before 2000, indicating the break points caused by instrument changes may lead to biases in the estimated trend and probably underes-

estimate the warming rate at the Chinese coast waters. Figure 4c also includes the SAT series during 1960–2015 for comparison. It

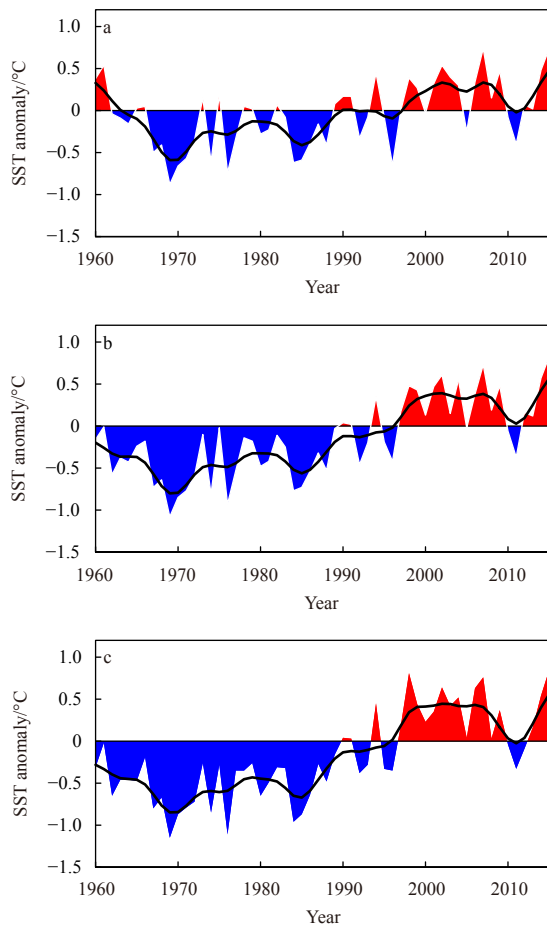


**Fig. 4.** Annual mean raw SST anomalies (a), homogenized SST anomalies (b) and homogenized SAT anomalies (c) averaged over the Chinese coast (1981–2010 base period). Gaussian low-pass filter is shown by the solid black line.

is obvious that the homogenized SST series and homogenized SAT series show much similar inter-annual variability as well as similar long-term trends ( $(0.22 \pm 0.06)^\circ\text{C}$  per decade for the SAT series).

The trends of the raw and homogenized annual mean SST series of stations along the Chinese coast are shown in Fig. 5. Obviously, both the raw and homogenized SST series of the 26 stations show warming trends; but the warming rates are much stronger in the homogenized data than those in the raw data in general. Results show that the warming was not spatially uniform along the Chinese coast. There were two rapid warming areas, that is, the northern East China Sea and the other area along the Bohai Sea, exceeding  $0.20^\circ\text{C}$  per decade. However, the spatial characteristic of warming cannot be found in the raw SST series (Fig. 5). About 14 SST series show significant increasing trends, exceeding  $0.18^\circ\text{C}$  per decade and most of these stations located in the north of the PTN station. The large-scale contrast of warming between north and south may have been primarily caused by the weakening East Asian Winter Monsoon (Committee on China's National Assessment Report on Climate Change, 2007; Ding, 2008), which generally exerted a larger influence in northern part of the coastal zone, and also partially caused by regional natural and human effects (Xie et al., 2002; Zhang et al., 2010; Park et al., 2015; Kako et al., 2016). However, further investigation is needed to better understand the spatial pattern of the SST increase.

In order to test the validity of the homogenized SST series, a SST dataset which has been widely used in the regional and global climate change studies is employed here for comparison. The SST dataset with  $0.25^\circ$  by  $0.25^\circ$  spatial resolution, called OISST which spans from 1982 to present. Firstly, OISST is interpolated to the stations' locations. Figure 6 includes the annual mean SST series in the coast of the China seas based on OISST during 1982–2015 for comparison with raw SST and homogenized SST respectively. It is notable that the annual mean homogenized SST series shows inter-annual variations very similar to that in the OISST (Fig. 6). The correlation coefficient calculated from Homogenized SST OISST is 0.87. However, there are discrepancies in the amplitudes between Raw SST and OISST (Fig. 6). The correlation coefficient calculated from Raw SST and OISST is 0.71 re-

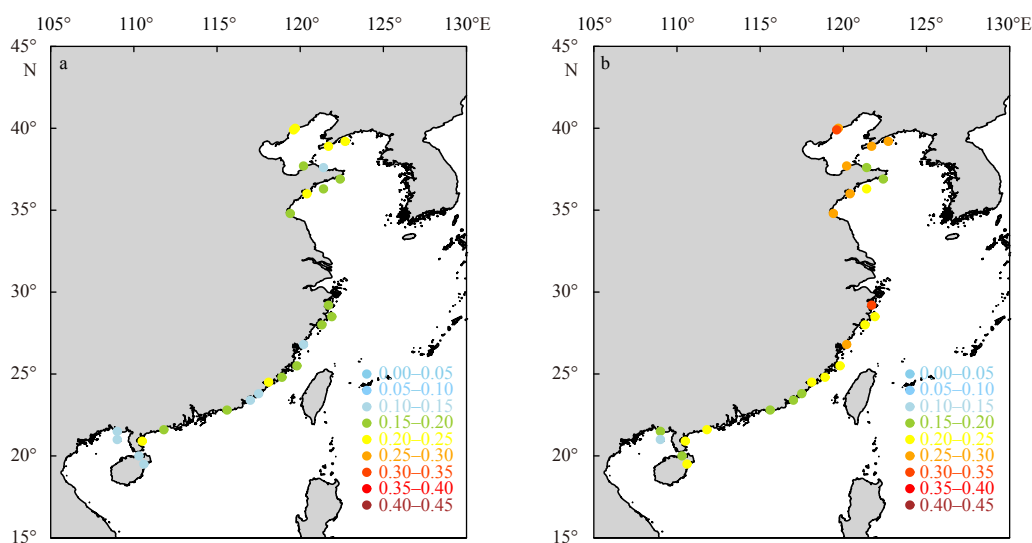


**Fig. 5.** Linear trends of annual mean original SST series (a) and homogenized SST series (b) during 1960–2015 at stations from north to south. The legend represents the temperature variation per decade, and the unit is  $^\circ\text{C}$ . See Table 1 and Fig. 1 for the full names and locations of the 26 coastal hydrological stations.

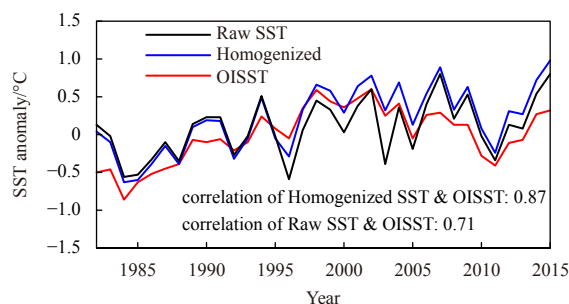


**Fig. 6.** Time series of the annual mean SST anomalies in the coast of the China seas from raw SST, homogenized SST, and OISST from 1982–2015 relative to the climate period of 1982–2010.

spectively which is lower than that from Homogenized SST. The result indicates that homogenized SST has a better consistency with the global gridded SST with high resolution than the raw SST in the coast area of China.

#### 4.3 Seasonal mean SST trends and atmospheric circulation variability

The homogenized SST series is more reliable than the raw SST series and thus could be used to assess the seasonal mean SST variabilities in this section. Previous studies of marginal sea of China found that the most significant warming rate occurred in winter and the slowest warming trend occurred in summer (Yeh and Kim, 2010; Bao and Ren, 2014). Thus, seasonal mean homogenized SST series for winter (December, January, and February) and summer (June, July, and August) were calculated. Trends of the two seasons were examined for individual station shown in Fig. 1. Clearly, most stations show robust SST warming trends in winter and weak warming trends in summer (Fig. 7). There was an asymmetric seasonal temperature trends in the Chinese coastal water in the past decades. More interestingly, the winter warming rates of each SST series increased with increasing latitude. These indicate that the warming rates were stronger

in winter than in summer and stronger in the relative cool area than in warm area during 1960–2015, which were consistent with previous reports of SAT changes in Chinese mainland (Chen et al., 2013; Li et al., 2015; Sun et al., 2018).

The general warming may have been mainly caused by anthropogenic increase in atmospheric CO<sub>2</sub> concentration and partly by the urbanization effect around the stations (Zhang et al., 2010). Considering the notable asymmetric seasonal trends and non-uniform spatial warming rate, however, the possible relationship between the largest warming rate occurring in winter and three large-scale atmospheric circulation modes were further analyzed. The AO index is often linked to winter climate variability in China and also correlated with the strength of the East Asian Winter Monsoon and Siberian high pressure system (Chen et al., 2013; You et al., 2013; Sun et al., 2018). It is notable that the winter AO index increases since the 1960s, accompanied by the weakening East Asian Winter Monsoon in general (Niu et al., 2010; He, 2013; Gong et al., 2018). The China seas are also generally influenced by East Asian Monsoon System and AO (Cai et al., 2017; Pei et al., 2017). Moreover, Yeh and Kim (2010) associated the increasing SST trends in the East China seas in winter with NPO-like sea level pressure change. They regarded the warming as driven by NPO mode through weakened northerly winds.

Figures 8a, c and e display the Pearson's correlation coefficients between the winter SST series in each station from north to south of the China seas and the atmospheric circulation indices. The winter EAT index may have exerted a major influence, as indicated by the high positive significant ( $p < 0.01$ ) correlations ( $r_1$ ) of 0.49–0.70 for all series. Yet, the winter AO index is only significantly and positively correlated with winter SST series at the coast of the Bohai Sea and Yellow Sea. Similarly, the winter NPO index is significantly and positively correlated with winter SST series at coast of the Yellow Sea and the East China Sea. Figure 8 also shows the annual and decadal mean circulation indices of EAT (Fig. 8b), AO (Fig. 8d) and NPO (Fig. 8f) from 1960 to 2015. It is notable that the winter EAT index has been consecutively increasing since the 1960s and transferred from negative phase (strong EAT) to positive phase (weak EAT) at the 1980s. Mean-

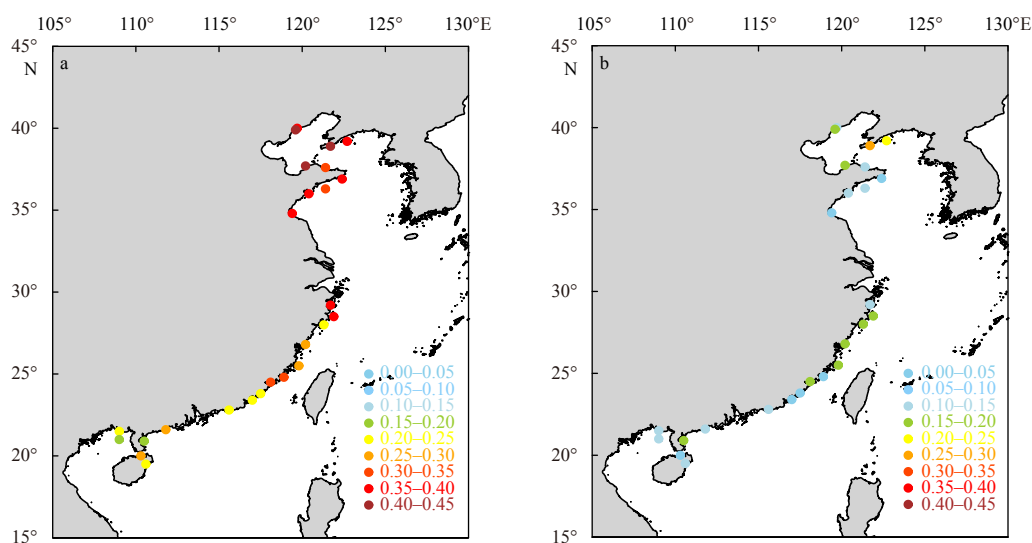


**Fig. 7.** Linear trends of seasonal mean SST in winter (a) and summer (b) at stations from north to south along the coast of China. The legend represents the temperature variation per decade, and the unit is °C. See Table 1 and Fig. 1 for the full names and locations of the 26 coastal hydrological stations.

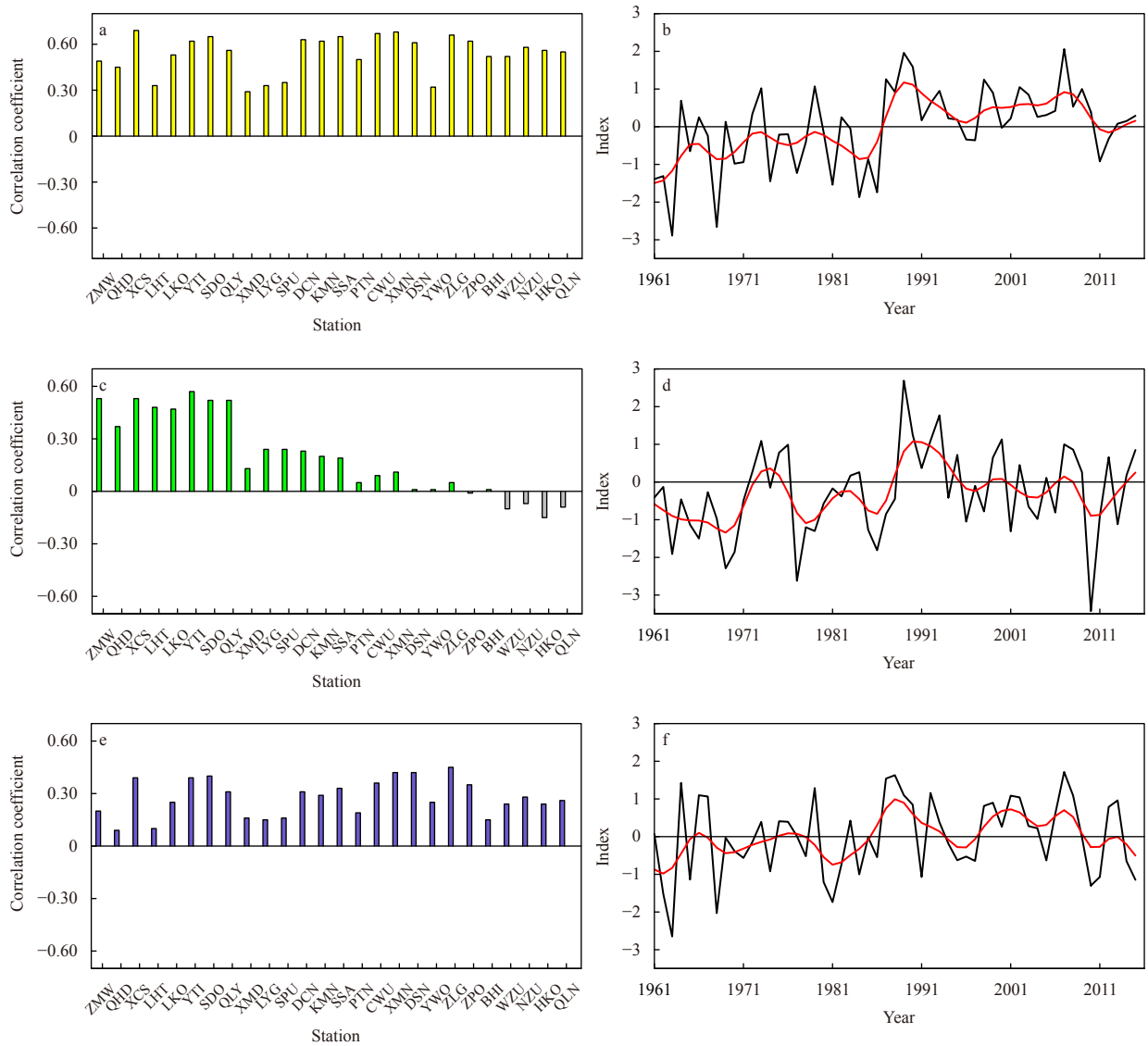


**Fig. 8.** Correlations between winter SST series at stations from north to south along the coast of China and the three atmospheric circulation indices: EAT index (a), AO index (c) and NPO index (e) (0.26 is the significant level at the 0.05 confidence level); and time series of winter EAT index (b), AO index (d) and NPO index (f) (black line). The smoother red line is the 9-year smoothing average for 1960–2015. See Table 1 and Fig. 1 for the full names and locations of the 26 coastal hydrological stations.

while, winter AO index has increased since the 1960s generally. NPO index also increased since 1960s, but the inter-annual variation amplitude is weaker than that of the other two indices.

It is clear that all of the three indices have an increasing trend since 1960s in general. The weaker EAT and stronger AO reduce the cold air of the polar region from entering into the China seas, especially north of the China seas. Moreover, NPO mode in higher phase weakened northerly winds. The circulation modes benefited the less frequent bursts of the winter cold waves and the sharp increase of winter SST in northern China seas during 1960–2015. Winter SST series at the northern China seas are possibly under the synergistic effects of EAT, AO and NPO from the middle-high latitude. This may well explain the more rapid and significant warming in winter at the northern China seas. In contrast, these atmospheric circulation modes exerted a relatively weak influence in winter SST series at the southern China seas, especially the AO.

#### 4.4 Some local effects

It is also possible that the SST observations themselves may have been affected by local tidal mixing, sea currents, fresh water discharge, urbanization and other kind of land use and land cover changes along the coastal zone, leading to locally heterogenous warming pattern. The more rapid warming along the Bohai Sea and the northern East China Sea as found in the Fig. 5b may have been related to the local factors in certain extents. The estuaries of the Changjiang River and the Huanghe River are located at the northern East China Sea and the Bohai Sea, respectively. Recently updated observations show that, from 1960 to 2015, the Changjiang River stably discharges fresh water of about 882 Gt each year (1960–2015 mean) to the East China Sea (Fig. 9a). Though, the Changjiang River discharge has shown no increasing trend, the stream water temperature in the Changjiang River Estuary increased by about 2.0°C since 1986 (Zhou et al., 2005), contributing to the extremely rapid warming observed in this sub-region.

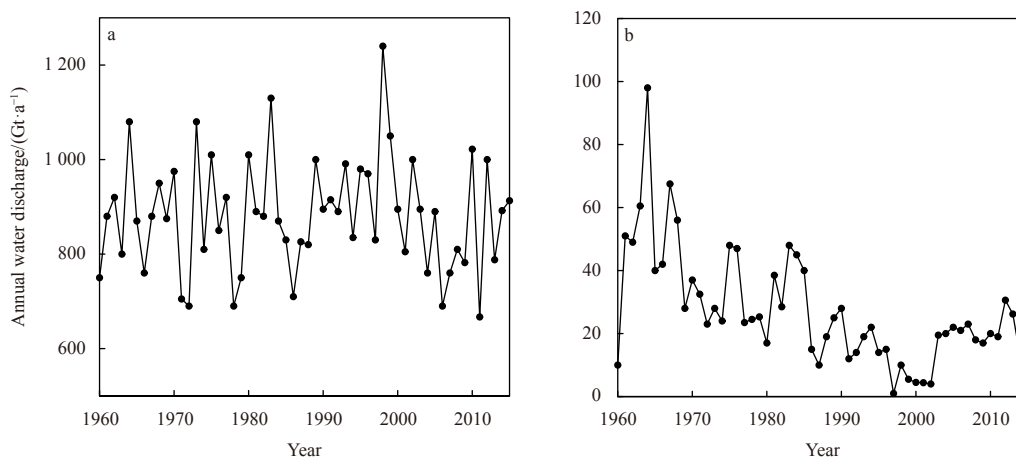


**Fig. 9.** Time series of the measured annual water discharge at Datong station of Changjiang River (31.8°N, 120.9°E) (a), and Lijin station (37.49°N, 118.25°E)<sup>①</sup> of the Huanghe River (b) from 1960 to 2015.

The rapid warming in the Bohai Sea might have had a different origin. As shown in Fig. 9b, the water discharge from the Huanghe River to the Bohai Sea has notably decreased from 1960 to 2015, with the rate of  $-0.68$  Gt/a. Considering that the Bohai Sea is the only inner sea of China which is surrounded by heavily populated and industrialized cities, the rapid warming in this sub-region might have resulted from the observed terrestrial warming affecting the adjacent coastal seas. Taken Dalian City (39°01'N, 121°44'E) as an example, the population grew from 1.28 million in 1953 to 6.69 million in 2010, at a 2.9% compound annual growth rate (the data source: reports of the National Census of China). Urbanization and the accompanying local warming may have contributed to the observed SST increase in some extents. The urbanization effect has been confirmed for annual and seasonal mean SAT trends in northern and eastern China (Ren et al., 2008, 2017; Yang et al., 2011), the observed SST trends along the Bohai Sea may have also been affected by urbanization. Therefore, the rapid warming along the Bohai Sea may have been partially caused by land-based anthropogenic activities, such as the local urbanization and the other kinds of land use and land cover change, in addition to the large-scale atmospheric circulation variability.

## 5 Discussion and conclusions

In this study, monthly mean SST recorded at 26 stations along the coast of the China seas from 1960 to 2015 have been homogenized, using the PMTred algorithm together with metadata to detect break points, and using the QM adjustment method conducted with reference series to adjust these series to diminish inhomogeneities.

It is notable that the instrument change including station system transformation is the main cause for the identified inhomogeneities, followed by stations relocation, accounting for about 61.3% and 24.2% of the total change points respectively. These artificial shifts in monthly SST series were then adjusted using the results of statistical tests together with available metadata. The ratio of the negative shifts is much higher than that of the positive shifts, indicating that homogenized SST largely corrects the

warm biases caused in the earlier artificial observing period. The warming rate of the whole SST series along the Chinese coast after adjustment is much larger than the raw data, up to  $0.19^{\circ}\text{C}$  per decade. Using the newly homogenized monthly mean SST data, seasonal mean SST trends in winter and summer were analyzed. Results show that the SST series located at the northern China seas have experienced robust warming trends in winter which are probably caused by the combined effect of multi-decadal variability of three large-scale atmospheric modes.

Due to the sparse of coastal hydrological stations in China, it is difficult to find an available SST series to make a reference sequence. In this case the SAT data as alternative data were used to construct the reference sequence. Based on the homogenized SST data, it is confirmed the rapid warming at the Chinese coast. The warming rate is comparable in magnitude to those reported in the eastern China based on SAT data (Ren et al., 2005, 2017) and in the China seas based on SST data (Bao and Ren, 2014) during the same period. The slightly lower warming trend of SST as compared to the increase of SAT along the coastal zone ( $(0.19 \pm 0.06)^{\circ}\text{C}$  per decade vs.  $(0.22 \pm 0.06)^{\circ}\text{C}$  per decade) may have been related to the fact that some of the SAT observations are made at urban stations, and the effect of urbanization on the estimated SAT trend may have been kept in the homogenized monthly mean SAT data series (Ren et al., 2008, 2015).

In this paper, the relationship between winter SST and several atmospheric circulation modes were analyzed. However, the dynamic linkage of the decadal and trend variation of the SST with oceanic oscillation modes and local oceanic forcing, such as Pacific Decadal Oscillation and El Niño–Southern Oscillation and Kuroshio Current, still needs to be investigated in future. In spite of the remaining issues mentioned above, this paper delivers the first results of SST data homogenization and the SST trend along the China seas based on the homogenized data of hydrological stations. The results are conducive to the understanding of regional climate change. The homogenized SST data could also be used as a benchmark for assessing the performance of analyses on globally gridded SST datasets.

<sup>①</sup> The two key gauge stations are used for monitoring the discharges of the Changjiang River and the Huanghe River (Zhang et al., 2014). The changes in the discharges at the two stations reflect the variations of the water fluxes from the two rivers to the sea. The data from the two gauge stations used in this study are collected from the Changjiang Water Conservancy Commission, the Huanghe River Conservancy Commission and the Bulletins of Chinese River Sediment.

### Acknowledgements

We thank Hamburg University's Cluster of Excellence CliSAP (Integrated Climate System Analysis and Prediction) for funding the visiting in Germany which benefits this study greatly.

### References

- Azorin-Molina C, Vicente-Serrano S M, McVicar T R, et al. 2014. Homogenization and assessment of observed near-surface wind speed trends over Spain and Portugal, 1961–2011. *Journal of Climate*, 27(10): 3692–3712, doi: [10.1175/JCLI-D-13-00652.1](https://doi.org/10.1175/JCLI-D-13-00652.1)
- Bao B, Ren Guoyu. 2014. Climatological characteristics and long-term change of SST over the marginal seas of China. *Continental Shelf Research*, 77: 96–106, doi: [10.1016/j.csr.2014.01.013](https://doi.org/10.1016/j.csr.2014.01.013)
- Belkin I M. 2009. Rapid warming of large marine ecosystems. *Progress in Oceanography*, 81(1–4): 207–213
- Cai Rongshuo, Tan Hongjian, Kontoyiannis H. 2017. Robust surface warming in offshore China seas and its relationship to the East Asian Monsoon wind field and ocean forcing on interdecadal time scales. *Journal of Climate*, 30(22): 8987–9005, doi: [10.1175/JCLI-D-16-0016.1](https://doi.org/10.1175/JCLI-D-16-0016.1)
- Cai Rongshuo, Tan Hongjian, Qi Qinghua. 2016. Impacts of and adaptation to inter-decadal marine climate change in coastal China seas. *International Journal of Climatology*, 36(11): 3770–3780, doi: [10.1002/joc.4591](https://doi.org/10.1002/joc.4591)
- Cao Lijuan, Zhao Ping, Yan Zhongwei, et al. 2013. Instrumental temperature series in eastern and central China back to the nineteenth century. *Journal of Geophysical Research: Atmospheres*, 118(15): 8197–8207, doi: [10.1002/jgrd.50615](https://doi.org/10.1002/jgrd.50615)
- Chen Shangfeng, Chen Wen, Wei Ke. 2013. Recent trends in winter temperature extremes in Eastern China and their relationship with the Arctic Oscillation and ENSO. *Advances in Atmospheric Sciences*, 30(6): 1712–1724, doi: [10.1007/s00376-013-2296-8](https://doi.org/10.1007/s00376-013-2296-8)
- Committee on China's National Assessment Report on Climate Change. 2007. *National Assessment Report on Climate Change* (in Chinese). Beijing: Science Press, 80–105
- Deser C, Alexander M A, Xie Shangping, et al. 2010. Sea surface temperature variability: patterns and mechanisms. *Annual Review of Marine Science*, 2: 115–143, doi: [10.1146/annurev-marine-120408-151453](https://doi.org/10.1146/annurev-marine-120408-151453)
- Ding Yihui. 2008. *Introduction to Climate Change Science of China* (in Chinese). Beijing: China Meteorological Press, 1–281
- Frölicher T L, Laufkötter C. 2018. Emerging risks from marine heat waves. *Nature Communications*, 9: 650, doi: [10.1038/s41467-018-03163-6](https://doi.org/10.1038/s41467-018-03163-6)
- Gong Hainan, Wang Lin, Chen Wen, et al. 2018. Multidecadal fluctuation of the wintertime Arctic Oscillation pattern and its implication. *Journal of Climate*, 31(14): 5595–5608, doi: [10.1175/JCLI-D-17-0530.1](https://doi.org/10.1175/JCLI-D-17-0530.1)
- Halpern B S, Walbridge S, Selkoe K A, et al. 2008. A global map of human impact on marine ecosystems. *Science*, 319(5865): 948–952, doi: [10.1126/science.1149345](https://doi.org/10.1126/science.1149345)
- Hansen J, Ruedy R, Sato M, et al. 2010. Global surface temperature change. *Reviews of Geophysics*, 48(4): RG4004, doi: [10.1029/2010RG000345](https://doi.org/10.1029/2010RG000345)
- Hausfather Z, Cowtan K, Menne M J, et al. 2016. Evaluating the impact of U.S. historical climatology network homogenization using the U.S. climate reference network. *Geophysical Research Letters*, 43(4): 1695–1701, doi: [10.1002/2015GL067640](https://doi.org/10.1002/2015GL067640)
- He Shengping. 2013. Reduction of the East Asian winter monsoon interannual variability after the mid-1980s and possible cause. *Chinese Science Bulletin*, 58(12): 1331–1338, doi: [10.1007/s11434-012-5468-5](https://doi.org/10.1007/s11434-012-5468-5)
- Huang Boyin, Liu Chunying, Banzon V F, et al. 2016. Assessing the impact of satellite-based observations in sea surface temperature trends. *Geophysical Research Letters*, 43(7): 3431–3437, doi: [10.1002/2016GL068757](https://doi.org/10.1002/2016GL068757)
- Kako S, Nakagawa T, Takayama K, et al. 2016. Impact of Changjiang River discharge on sea surface temperature in the East China Sea. *Journal of Physical Oceanography*, 46(6): 1735–1750, doi: [10.1175/JPO-D-15-0167.1](https://doi.org/10.1175/JPO-D-15-0167.1)
- Kalnay E, Kanamitsu R, Kistler W, et al. 1996. The NCEP/NCAR 40-year reanalysis project. *Bulletin of the American Meteorological Society*, 77(3): 437–472, doi: [10.1175/1520-0477\(1996\)077<0437:TNYRP>2.0.CO;2](https://doi.org/10.1175/1520-0477(1996)077<0437:TNYRP>2.0.CO;2)
- Kuglitsch F G, Auchmann R, Bleisch R, et al. 2012. Break detection of annual Swiss temperature series. *Journal of Geophysical Research: Atmospheres*, 117(D13): D13105, doi: [10.1029/2012JD017729](https://doi.org/10.1029/2012JD017729)
- Li Yan, Mu Lin, Wang Guosong, et al. 2016. The detecting and adjusting of the sea surface temperature data homogeneity over coastal zone of circum Bohai Sea. *Haiyang Xuebao* (in Chinese), 38(3): 27–39
- Li Yan, Mu Lin, Wang Qingyuan, et al. 2020. High-quality sea surface temperature measurements along coast of the Bohai and Yellow seas in China and their long-term trends during 1960–2012. *International Journal of Climatology*, 40(1): 63–76, doi: [10.1002/joc.6194](https://doi.org/10.1002/joc.6194)
- Li Qingxiang, Yang Su, Xu Wenhui, et al. 2015. China experiencing the recent warming hiatus. *Geophysical Research Letters*, 42(3): 889–898, doi: [10.1002/2014GL062773](https://doi.org/10.1002/2014GL062773)
- Li Qingxiang, Zhang Hongzheng, Liu Xiaoning, et al. 2009. A mainland China homogenized historical temperature dataset of 1951–2004. *Bulletin of the American Meteorological Society*, 90(8): 1062–1066, doi: [10.1175/2009BAMS2736.1](https://doi.org/10.1175/2009BAMS2736.1)
- Lima F P, Wetthey D S. 2012. Three decades of high-resolution coastal sea surface temperatures reveal more than warming. *Nature Communications*, 3: 704, doi: [10.1038/ncomms1713](https://doi.org/10.1038/ncomms1713)
- Linkin M E, Nigam S. 2008. The North Pacific oscillation-West Pacific teleconnection pattern: mature-phase structure and winter impacts. *Journal of Climate*, 21(9): 1979–1997, doi: [10.1175/2007JCLI2048.1](https://doi.org/10.1175/2007JCLI2048.1)
- Malcher J, Schönwiese C D. 1987. Homogeneity, spatial correlation and spectral variance analysis of long European and North American air temperature records. *Theoretical and Applied Climatology*, 38(3): 157–166, doi: [10.1007/BF00868100](https://doi.org/10.1007/BF00868100)
- Minola L, Azorin-Molina C, Chen Deliang. 2016. Homogenization and assessment of observed near-surface wind speed trends across Sweden, 1956–2013. *Journal of Climate*, 29(20): 7397–7415, doi: [10.1175/JCLI-D-15-0636.1](https://doi.org/10.1175/JCLI-D-15-0636.1)
- Niu Feng, Li Zhanqing, Li Can, et al. 2010. Increase of wintertime fog in China: potential impacts of weakening of the Eastern Asian monsoon circulation and increasing aerosol loading. *Journal of Geophysical Research: Atmospheres*, 115(D7): D00K20, doi: [10.1029/2009jd013484](https://doi.org/10.1029/2009jd013484)
- Park K A, Lee E Y, Chang E, et al. 2015. Spatial and temporal variability of sea surface temperature and warming trends in the Yellow Sea. *Journal of Marine Systems*, 143: 24–38, doi: [10.1016/j.jmarsys.2014.10.013](https://doi.org/10.1016/j.jmarsys.2014.10.013)
- Pei Yuhua, Liu Xiaohui, He Hailun. 2017. Interpreting the sea surface temperature warming trend in the Yellow Sea and East China Sea. *Science China Earth Sciences*, 60(8): 1558–1568, doi: [10.1007/s11430-017-9054-5](https://doi.org/10.1007/s11430-017-9054-5)
- People's Republic of China National Bureau of Technical Supervision. 2006. GB/T 14914-2006 The specification for offshore observation (in Chinese). Beijing: China Standards Press, 1–83
- Reeves J, Chen Jien, Wang Xiaolan, et al. 2007. A review and comparison of changepoint detection techniques for climate data. *Journal of Applied Meteorological and Climatology*, 46(6): 900–915, doi: [10.1175/JAM2493.1](https://doi.org/10.1175/JAM2493.1)
- Ren Guoyu, Ding Yihui, Tang Guoli. 2017. An overview of Mainland China temperature change research. *Journal of Meteorological Research*, 31(1): 3–16, doi: [10.1007/s13351-017-6195-2](https://doi.org/10.1007/s13351-017-6195-2)
- Ren Guoyu, Guo Jun, Xu Mingzhi, et al. 2005. Climate changes of China's mainland over the past half century. *Acta Meteorologica Sinica* (in Chinese), 63(6): 942–956
- Ren Guoyu, Li Jiao, Ren Yuyu, et al. 2015. An integrated procedure to determine a reference station network for evaluating and adjusting urban bias in surface air temperature data. *Journal of Applied Meteorology and Climatology*, 54(6): 1248–1266, doi: [10.1175/JAMC-D-14-0295.1](https://doi.org/10.1175/JAMC-D-14-0295.1)
- Ren Guoyu, Zhang Aiyang, Chu Ziyang, et al. 2010. Principles and pro-

- cedures for selecting reference surface air temperature stations in China. *Meteorological Science and Technology* (in Chinese), 38(1): 78–85
- Ren Guoyu, Zhou Yaqing, Chu Ziyang, et al. 2008. Urbanization effects on observed surface air temperature trends in north China. *Journal of Climate*, 21(6): 1333–1348, doi: [10.1175/2007JCLI1348.1](https://doi.org/10.1175/2007JCLI1348.1)
- Reynolds R W, Smith T M, Liu Chunying, et al. 2007. Daily high-resolution-blended analyses for sea surface temperature. *Journal of Climate*, 20(22): 5473–5496, doi: [10.1175/2007JCLI1824.1](https://doi.org/10.1175/2007JCLI1824.1)
- Ribeiro S, Caineta J, Costa A C. 2015. Review and discussion of homogenisation methods for climate data. *Physics and Chemistry of the Earth, Parts A/B/C*, 94: 167–179, doi: [10.1016/j.pce.2015.08.007](https://doi.org/10.1016/j.pce.2015.08.007)
- Sen P K. 1968. Estimates of the regression coefficient based on Kendall's tau. *Journal of the American Statistical Association*, 63(324): 1379–1389, doi: [10.1080/01621459.1968.10480934](https://doi.org/10.1080/01621459.1968.10480934)
- Stephenson T S, Goodess C M, Haylock M R, et al. 2008. Detecting inhomogeneities in Caribbean and adjacent Caribbean temperature data using sea-surface temperatures. *Journal of Geophysical Research: Atmospheres*, 113(D21): D21116, doi: [10.1029/2007JD009127](https://doi.org/10.1029/2007JD009127)
- Stramska M, Białogrodzka J. 2015. Spatial and temporal variability of sea surface temperature in the Baltic Sea based on 32-years (1982–2013) of satellite data. *Oceanologia*, 57(3): 223–235, doi: [10.1016/j.oceano.2015.04.004](https://doi.org/10.1016/j.oceano.2015.04.004)
- Sun Xiangping. 2006. *China Offshore Area* (in Chinese). Beijing: China Ocean Press, 97–120
- Sun Baimin, Li Chongyin. 1997. Relationship between disturbance of East Asian trough and tropical convection activities. *Chinese Science Bulletin* (in Chinese), 42(5): 500–504
- Sun Xiubao, Ren Guoyu, Ren Yuyu, et al. 2018. A remarkable climate warming hiatus over northeast China since 1998. *Theoretical and Applied Climatology*, 133(1): 579–594, doi: [10.1007/s00704-017-2205-7](https://doi.org/10.1007/s00704-017-2205-7)
- Thompson D W J, Wallace J M. 1998. The Arctic oscillation signature in the wintertime geopotential height and temperature fields. *Geophysical Research Letters*, 25(9): 1297–1300, doi: [10.1029/98GL00950](https://doi.org/10.1029/98GL00950)
- Vincent L A, Wang Xiaolan, Milewska E J, et al. 2012. A second generation of homogenized Canadian monthly surface air temperature for climate trend analysis. *Journal of Geophysical Research: Atmospheres*, 117(D18): D18110, doi: [10.1029/2012JD017859](https://doi.org/10.1029/2012JD017859)
- Wan Hui, Wang Xiaolan, Swail V R. 2010. Homogenization and trend analysis of Canadian near-surface wind speeds. *Journal of Climate*, 23(5): 1209–1225, doi: [10.1175/2009JCLI3200.1](https://doi.org/10.1175/2009JCLI3200.1)
- Wang Xiaolan. 2008a. Accounting for autocorrelation in detecting mean shifts in climate data series using the penalized maximal t or F test. *Journal of Applied Meteorology and Climatology*, 47(9): 2423–2444, doi: [10.1175/2008JAMC1741.1](https://doi.org/10.1175/2008JAMC1741.1)
- Wang Xiaolan. 2008b. Penalized maximal F test for detecting undocumented mean shift without trend change. *Journal of Atmospheric and Oceanic Technology*, 25(3): 368–384, doi: [10.1175/2007JTECHA982.1](https://doi.org/10.1175/2007JTECHA982.1)
- Wang Xiaolan, Chen Hanfeng, Wu Yuehua, et al. 2010. New techniques for the detection and adjustment of shifts in daily precipitation data series. *Journal of Applied Meteorology and Climatology*, 49(12): 2416–2436, doi: [10.1175/2010jamc2376.1](https://doi.org/10.1175/2010jamc2376.1)
- Wang Xiaolan, Feng Yang. 2013. *RHtestsV4 user manual*. Toronto, Ontario, Canada: Environment Canada
- Wang Xiaolan, Wen Qiuhan, Wu Yuehua. 2007. Penalized maximal t test for detecting undocumented mean change in climate data series. *Journal of Applied Meteorology and Climatology*, 46(6): 916–931, doi: [10.1175/JAM2504.1](https://doi.org/10.1175/JAM2504.1)
- Xie Shangping, Hafner J, Tanimoto Y, et al. 2002. Bathymetric effect on the winter sea surface temperature and climate of the Yellow and East China seas. *Geophysical Research Letter*, 29(24): 2228, doi: [10.1029/2002GL015884](https://doi.org/10.1029/2002GL015884)
- Xu Wenhui, Li Qingxang, Wang Xiaolan, et al. 2013. Homogenization of Chinese daily surface air temperatures and analysis of trends in the extreme temperature indices. *Journal of Geophysical Research: Atmosphere*, 118(17): 9708–9720, doi: [10.1002/jgrd.50791](https://doi.org/10.1002/jgrd.50791)
- Yang Xuchao, Hou Yiling, Chen Baode. 2011. Observed surface warming induced by urbanization in East China. *Journal of Geophysical Research: Atmospheres*, 116(D14): D14113, doi: [10.1029/2010JD015452](https://doi.org/10.1029/2010JD015452)
- Yang Su, Wang Xiaolan, Wild M. 2018. Homogenization and trend analysis of the 1958–2016 In Situ surface solar radiation records in China. *Journal of Climate*, 31(11): 4529–4541, doi: [10.1175/JCLI-D-17-0891.1](https://doi.org/10.1175/JCLI-D-17-0891.1)
- Yeh S W, Kim C H. 2010. Recent warming in the Yellow/East China Sea during winter and the associated atmospheric circulation. *Continental Shelf Research*, 30(13): 1428–1434, doi: [10.1016/j.csr.2010.05.002](https://doi.org/10.1016/j.csr.2010.05.002)
- You Qinglong, Ren Guoyu, Fraedrich K, et al. 2013. Winter temperature extremes in China and their possible causes. *International Journal of Climatology*, 33(6): 1444–1455, doi: [10.1002/joc.3525](https://doi.org/10.1002/joc.3525)
- Zhang Lei, Ren Guoyu, Ren Yuyu, et al. 2014. Effect of data homogenization on estimate of temperature trend: a case of Huairou station in Beijing Municipality. *Theoretical and Applied Climatology*, 115(3): 365–373, doi: [10.1007/s00704-013-0894-0](https://doi.org/10.1007/s00704-013-0894-0)
- Zhang Liping, Wu Lixin, Lin Xiaopei, et al. 2010. Modes and mechanisms of sea surface temperature low-frequency variations over the coastal China seas. *Journal of Geophysical Research: Oceans*, 115(C8): C08031, doi: [10.1029/2009JC006025](https://doi.org/10.1029/2009JC006025)
- Zhou Xiaoying, Hu Debao, Wang Cizhen, et al. 2005. Seasonal and interannual SST variations in the Changjiang Estuary. *Periodical of Ocean University of China* (in Chinese), 35(3): 357–362